

# TRACKS WITH UNDER-BALLAST PLATES AND THEIR MITIGATION OF TRAIN INDUCED GROUND VIBRATION

Lutz Auersch

*Federal Institute of Material Research and Testing, Berlin (BAM), Germany*  
email: lutz.auersch-saworski@bam.de

Experiments have been performed at a test site with six different tracks with under-ballast plates. Hammer excitations of the soil and the tracks as well as train passages have been measured. The experimental observations are as follows. 1. The natural soil is stiff gravel whereas the railway dam consists of softer material. 2. The track compliance indicates a soft ballast if no train is present to provide a confining pressure. 3. The track response to the train passages can be split into a low-frequency region which is ruled by the static loads and a high-frequency region which is ruled by dynamic loads. 4. The track responses to hammer and track excitation indicate the presence of many voids between the sleepers and the ballast. 5. The ground vibrations are highly influenced by the soil. Due to the stiff soil at the site, the hammer and train induced spectra have a considerable high-frequency content. 6. A reduction of the ground vibration has been observed in a low-frequency range. The mitigation effects of an under-ballast plate are also investigated by calculations of a wavenumber domain model. The under-ballast plate has an effect at low frequencies where it distributes the static load over a longer track section. The impulse of the axle passage is longer and the frequencies are lower due to the plate stiffness. The axle impulses could yield a low-frequency ground vibration in an irregular soil with a randomly varying stiffness. This low-frequency part of the ground vibration (the scattered axle impulses) seem to be reduced by the under-ballast plate.

---

Keywords: railway vibration, ballast tracks, under-ballast plate, ground vibration

---

## 1. Introduction to the measurements at the Altheim site

At Altheim in South Germany, six track sections have been built, one reference ballast track section and five track sections with under-ballast plates with or without under-ballast mats. The principal structure of the track is presented in Figure 1. The rail at the Altheim test site is a S54 rail the sleepers are B70 sleepers lying in a distance of 0.6 m. The ballast is  $h_B = 0.3$  m, the concrete plate  $h_P = 0.3$  m thick.

Early measurements have been performed at one free-field point in 8 m distance from each track to establish the mitigation of train-induced ground vibration. The measured differences between the different tracks were difficult to explain [1]. It was concluded that the soil at these track sections must be analysed in more detail and that theoretical models are necessary to understand the differences. BAM has performed detailed measurements at Altheim (and two more places) as part of a research work on the prediction of train induced ground vibration [2]. The methods necessary for the prediction and the results are presented in the following contribution.

The measured and calculated results about the mitigation effects are presented for an under-ballast plate, but similar results have also been obtained for an under-ballast mat and may be expected for under-sleeper pads. The present contribution concentrates on what has been measured at the Altheim site: the under-ballast plate.

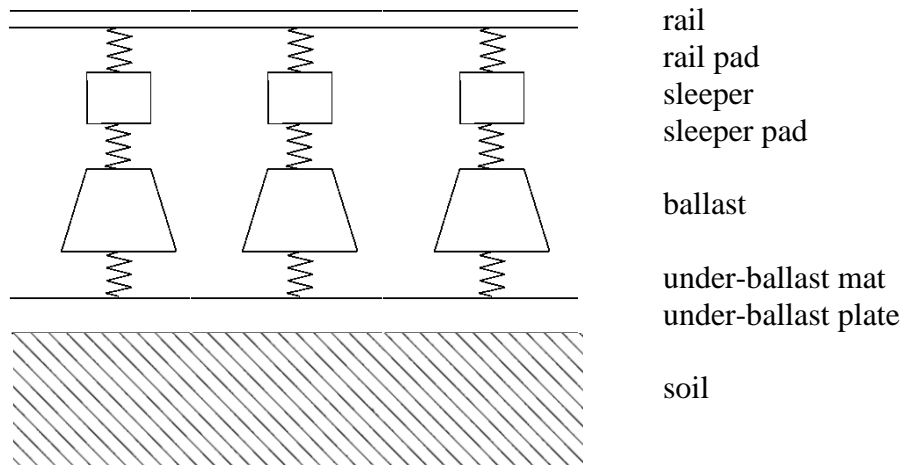


Figure 1: Track model consisting of rail, rail pad, sleeper, under-sleeper pad, ballast, under-ballast mat, under-ballast plate and continuous soil model.

## 2. Experiments to characterize the soil

### 2.1 Wave velocities of the soil

The soil of the test site has been analysed by hammer impacts. The hammer impacts generate waves through the soil. The response of the soil is measured by geophones which are placed equidistant in a measuring line. The measuring line is usually perpendicular to the track if the soil for the propagation of the train induced ground vibration is of interest, but if the sub-soil of the track structure is of interest, a measuring line lies close to and parallel to the track. Both measuring lines have been used in Altheim, and the wave propagation along the track is measured twice, on the soil and on the sleepers. Figure 2 shows the time histories of all measuring points due to a hammer impact on the sleeper. The propagation of the main impulse can be observed as the on-set of the low frequency vibration with a wave velocity of about 300 m/s. These low-frequency vibration becomes considerably longer at the further measuring points. The first arrival of waves consists of much higher frequencies. Altogether, these characteristics describe a dispersive nature of the track-soil system, where the bending stiffness of the track results in faster waves at higher frequencies (abnormal dispersion).

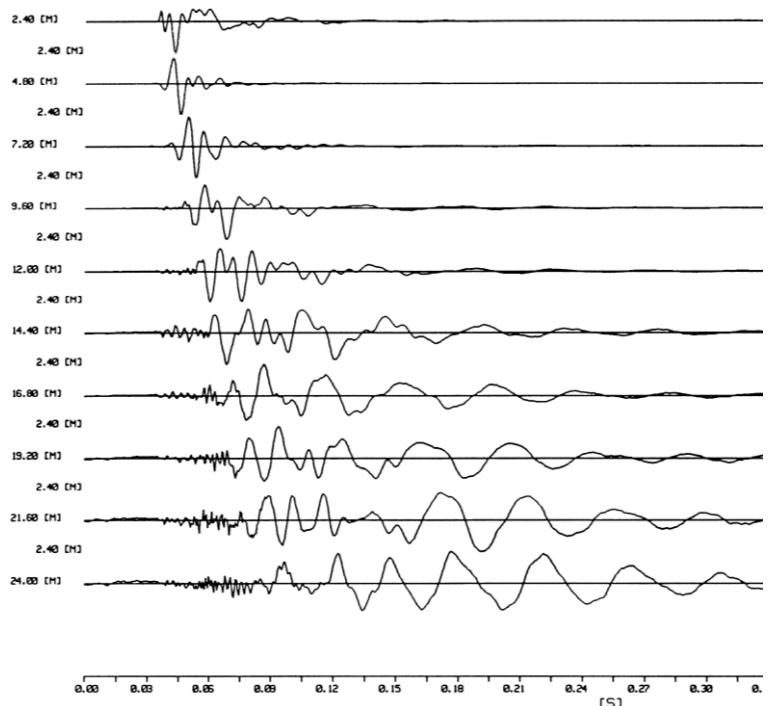


Figure 2: Wave propagation through the sub-soil of the track, hammer excitation on a sleeper.

The frequency-dependent wave velocities can be analysed by different methods such as SASW, MASW, wavenumber analysis, and SPAC [3]. Figure 3 shows the results of a special Multistation Analysis of Surface Wave method (MASW). The phase spectra of all responses compared to the impact force spectrum are unwrapped and plotted. For each frequency, the phases are approximated by linear phase-distance function which determines the wave velocity at this frequency. A smaller

phase difference per frequency means a higher velocity. Figure 3b shows the results for the sub-soil of the track where the wave velocities increase with frequency (abnormal dispersion). The phase curves for the free-field soil in Figure 3a are bent down indicating that the phase differences per frequency become greater and the wave velocity lower with increasing frequency (normal dispersion, typical for a natural soil).

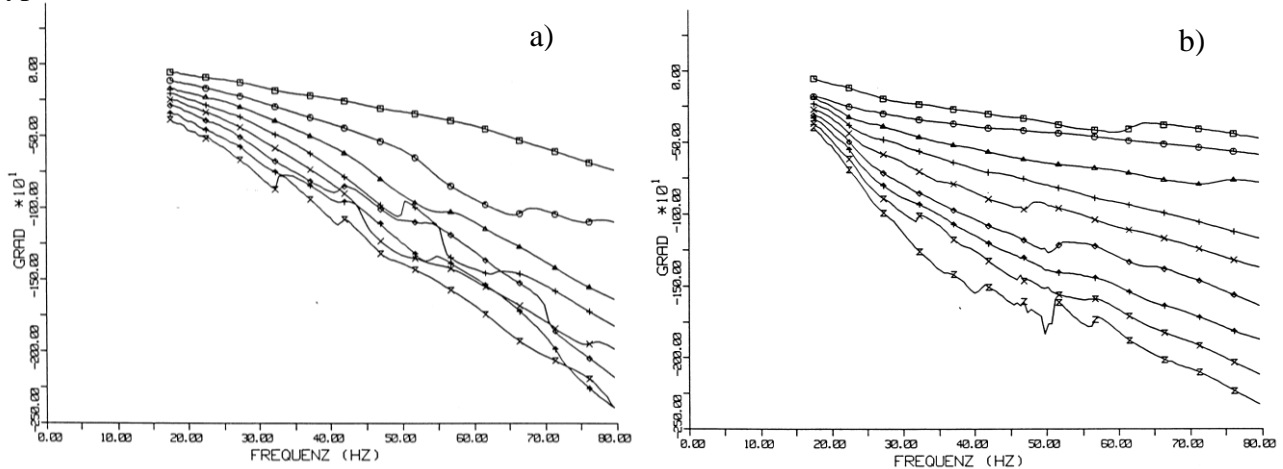


Figure 3: Phase spectra of the transfer functions indicating a) a normal dispersion of the free-field soil and b) an abnormal dispersion of the track sub-soil.

## 2.2 Transfer functions of the stiff soil

The impact results of the measuring axes can also be evaluated for the transfer function of the soil. The mobilities (particle velocity spectra divided by the force spectrum) are presented for the near- and far-field points as one-third of octave band spectra (Fig. 4a). This presentation can also help to identify the soil structure at a site. The measured results show an increase with frequency up to high frequencies. The ratio between the nearest and the furthest point describes the attenuation of the ground vibration with distance. It is relatively small, less than a factor 10 below 20 Hz and less than 100 at high frequencies. These characteristics are typical for a stiff soil with little damping. Figure 4b shows a theoretical transfer function for a soil with a shear wave velocity of  $v_s = 300$  m/s and a material damping of  $D = 2.5\%$  for comparison.

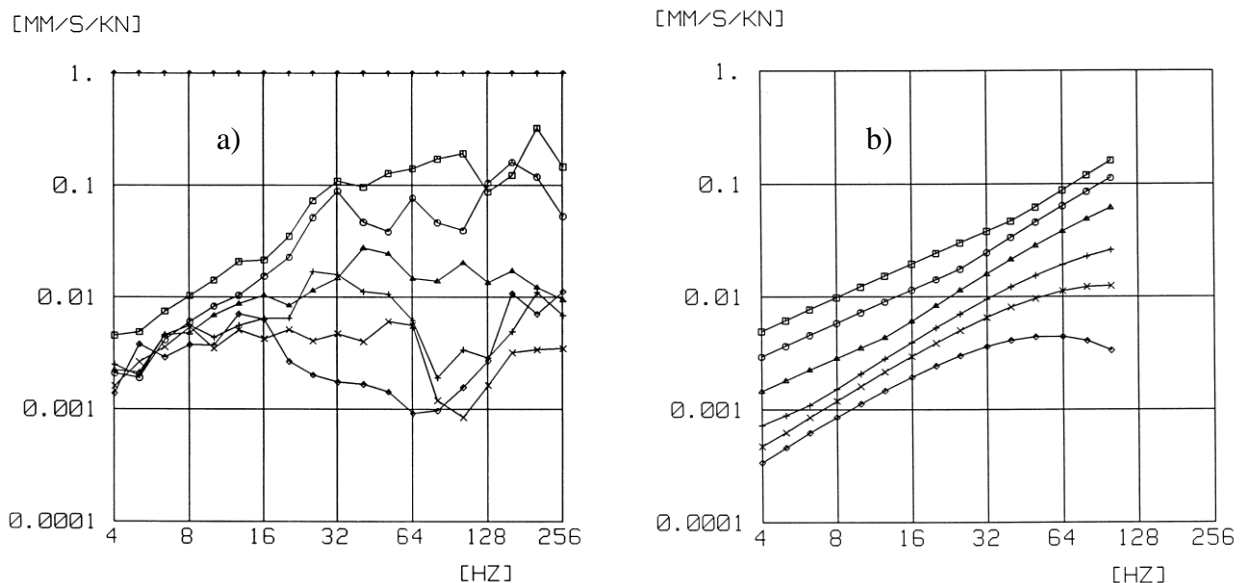


Figure 4: Measured (a) and calculated (b) transfer function of the soil at  $r = \square 3, \circ 5, \triangle 10, + 20, \times 30, \diamond 50$  m, calculation for a homogeneous soil of  $v_s = 300$  m/s and  $D = 2.5\%$ .

### 3. Response of the track to hammer and train load

Hammer impacts on the rail have been evaluated for the frequency-dependent compliance functions of the track (Fig. 5). The compliances of the six track sections vary considerably. Moreover, some compliances are rather great compared to the theory in [4]. Even impacts above two consecutive sleepers showed different results. Therefore, it has been concluded that the ballast is rather soft if no train is stiffening it by its weight, and that many voids exist between the sleepers and the ballast.

This conclusion has been confirmed by the results from the train passages. Figure 6 shows for example the rail and sleeper displacements and velocities when a locomotive and one and a half carriage are passing track 6 with 100 km/h. The track displacements are evaluated from the measured track velocities after filtering out the high-frequency content [4], and they present the static compliance of the track. The unfiltered velocity time records (Fig. 6b) include the low-frequency axle impulses as well as a high-frequency noise. The corresponding one-third octave band spectra are shown in Figure 8a for all six track sections. The spectra are divided in two parts, a low-frequency part up to 20 Hz which is quite similar for all tracks, and a high-frequency part, which seems to be related to the track state. Those tracks which showed a high compliance (for example track 3 and 5) show also a stronger high-frequency train induced vibration [5].

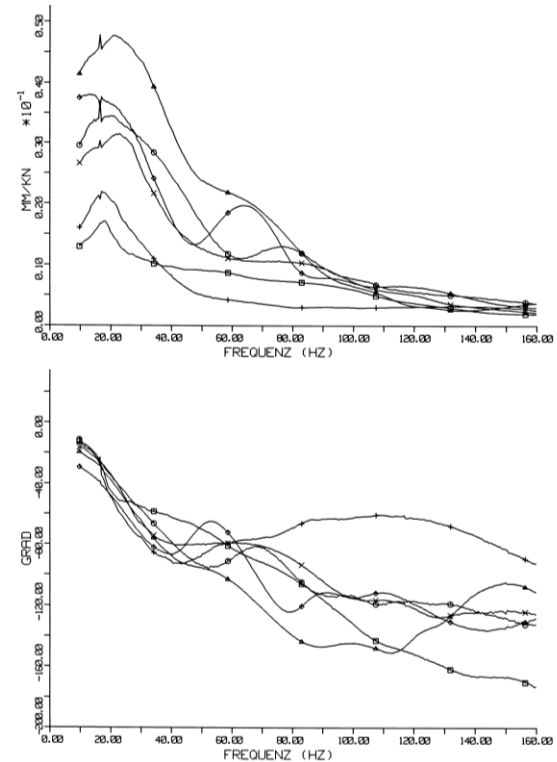


Figure 5: Amplitude and phase of the transfer functions of the different track sections  $\square$  1,  $\circ$  2,  $\triangle$  3,  $+$  4,  $\times$  5,  $\diamond$  6.

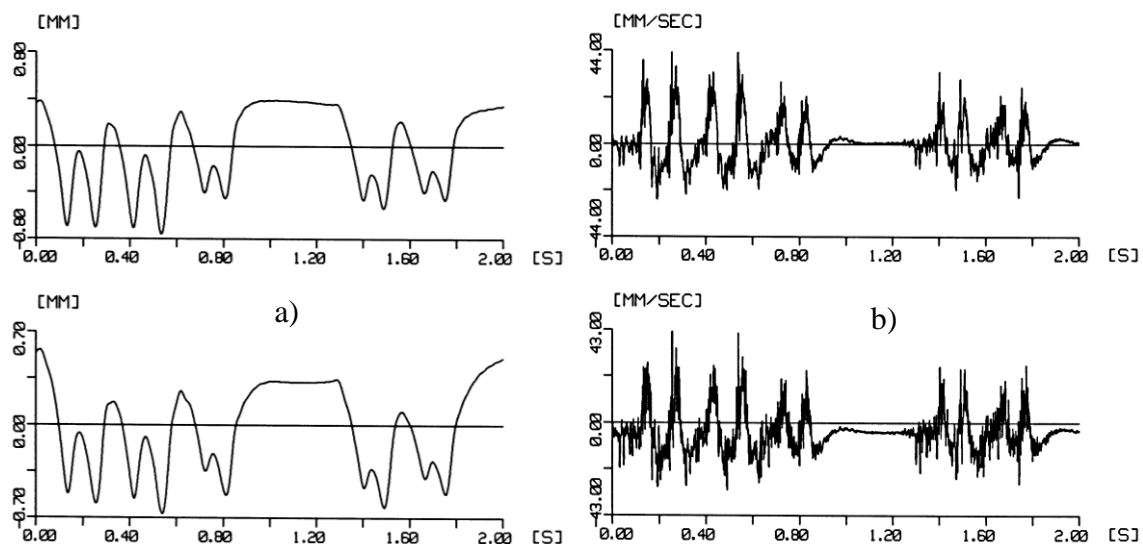


Figure 6: Track response to train passage, a) rail and sleeper displacements, b) rail and sleeper velocities; time histories at track 6,

## 4. Measured train-induced ground vibration and the mitigation effect of the under-ballast plate

### 4.1 Response of the soil to hammer impact and train passages

The train induced ground vibration are presented as one-third of octave band spectra for near and far-field points (Fig. 7c,d). The same measuring points have been evaluated for the hammer impacts on the rail (Fig. 7a,b). Hammer and train results have common characteristics. The near-field points have high amplitudes in the mid-frequency range whereas the far-field points show small and nearly constant spectra in agreement with the free-field spectra in Figure 4a. The near-field spectra look like a soft soil with a low-frequency cut-off due to increasing stiffness with depth, a high-frequency cut-off due to the strong effect of damping, and an elevated mid-frequency region. The difference between the soft near-field and the stiff far-field behavior can be explained by the artificial dam in the near-field where soft material has been tipped on the natural stiff soil.

The similarity of the hammer and train-induced spectra proves the reasonable use of the hammer excitation for the prediction of train induced ground vibration [2]. Moreover, a rather smooth force spectrum can be concluded [5]. The only singular frequency component is the sleeper passing frequency of 50 Hz.

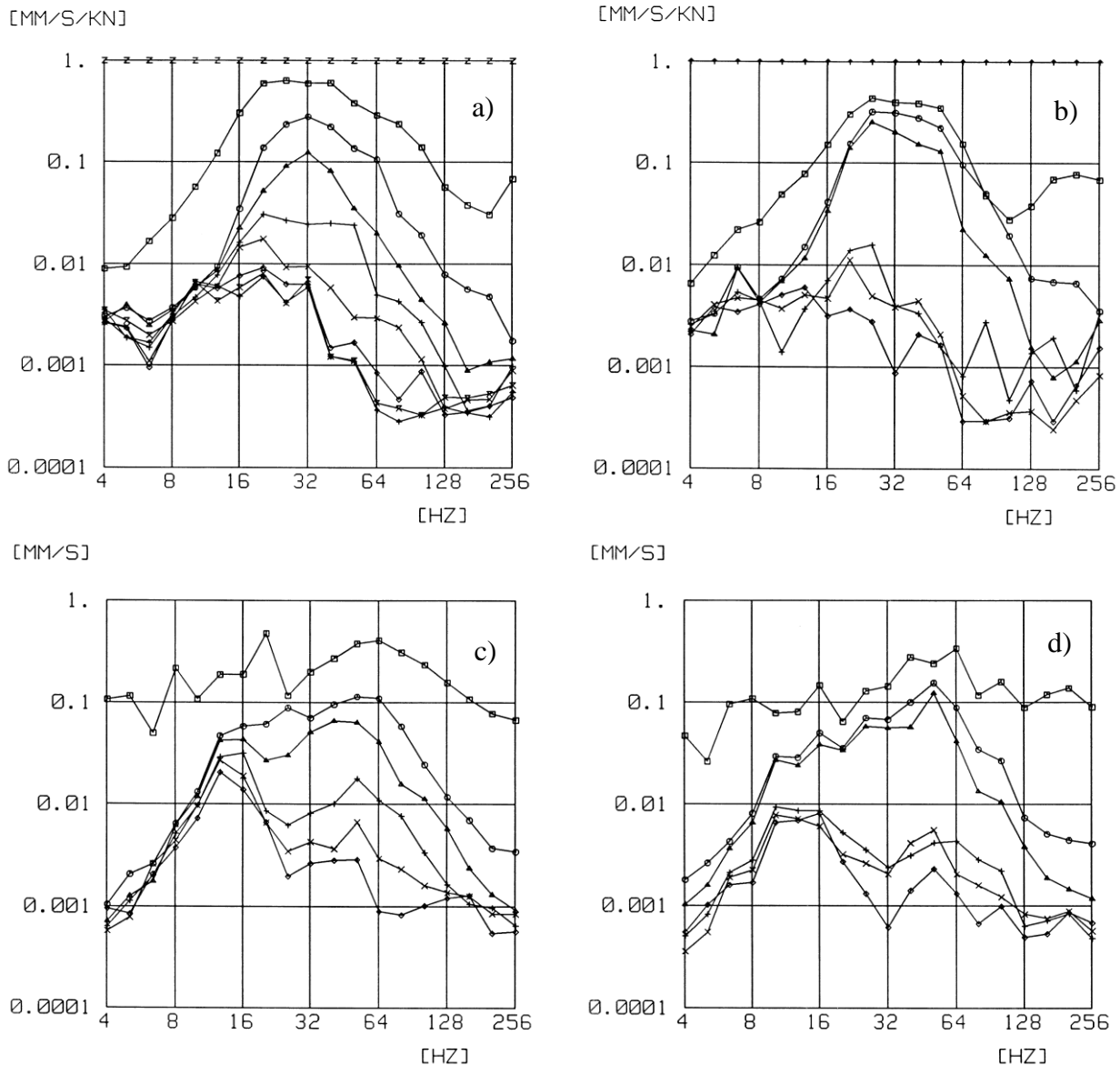


Figure 7: Ground vibration due to a,b) hammer and c,d) train excitation, a,c) track 1 without plate, b,d) track 2 with plate,  $r = \square$  2,  $\circ$  7,  $\triangle$  10,  $+$  20,  $\times$  30,  $\diamond$  50 m.



## 4.2 Comparison of the sections with and without ballast plate

The comparison of the ground vibration strongly depends on the distance to the track. At the near-field points on the dam, the results are quite arbitrary with unexpected high amplitudes at track II. The irregularities occur for the hammer and for the train excitation as well. These irregularities explain why the mitigation of ground vibration by the different ballast-plate tracks could not be established from the near-field points [1]. Knowledge about the soil is very important if different track sections should be compared.

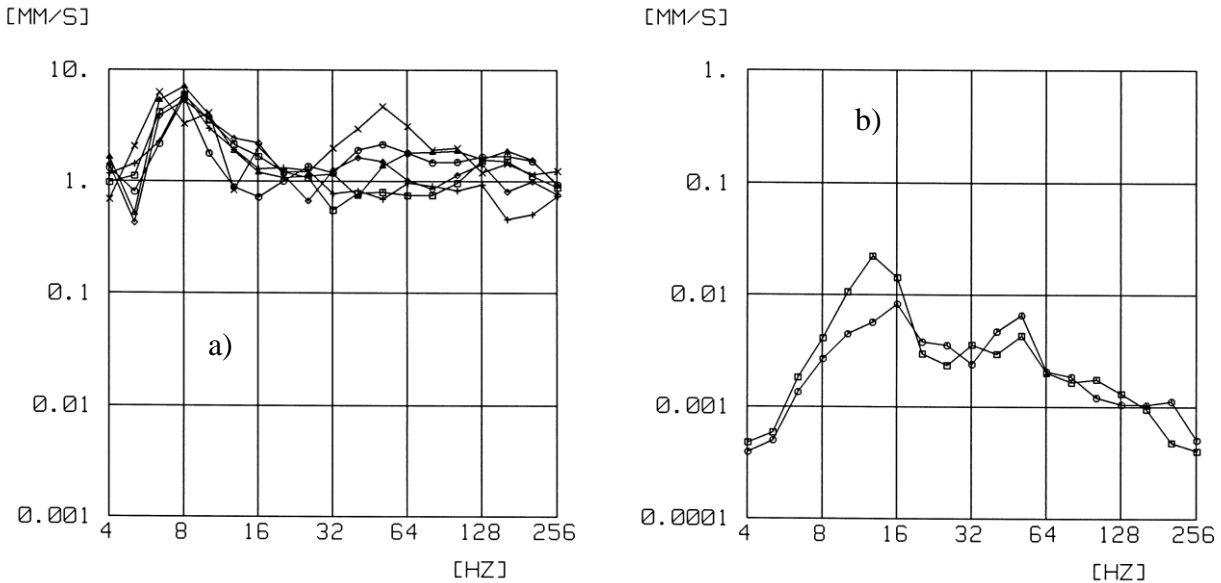


Figure 8: Train-induced track vibration at track sections  $\square$  1,  $\circ$  2,  $\triangle$  3,  $+$  4,  $\times$  5,  $\diamond$  6 (a) and ground vibration at 30 m distance from the track,  $\square$  track 1 without plate,  $\circ$  track 2 with plate.

Nevertheless, the results of the complete measuring axes can be evaluated for the effects of the different tracks. If we look at the far-field results which are from the regular natural soil, a clear difference can be found at a certain raised vibration component around 10 Hz. The amplitudes for the track with under ballast plate are clearly smaller than the amplitudes of the reference track without plate. The results at  $r = 30$  m are directly compared in Figure 8b and the strongest reduction has been found as one fourth (-12 dB) at 12 Hz.

## 5. Calculation of ballast-plate tracks in wavenumber domain

The ballast-plate track model of Figure 1 is calculated in frequency wavenumber domain [7]. The following parameters have been chosen, bending stiffness of the S54 rails  $EI_R = 2 \times 2.1 \cdot 10^{11} \times 2.3 \cdot 10^{-5} \text{ Nm}^2 = 9.7 \cdot 10^6 \text{ Nm}^2$ , mass per length of the rails  $m'_R = 2 \times 54 \text{ kg/m}$ , stiffness of the ballast  $k_B = 2.6 \cdot 10^9 \text{ N/m}$ , shear wave velocity of the soil  $v_S = 300 \text{ m/s}$ . Results are presented for four different track systems, a reference ballast track without plate, a track with a thin under-ballast plate ( $h_P = 0.15 \text{ m}$ ), a track with a thick under-ballast plate ( $h_P = 0.5 \text{ m}$ ) and a track with a plate of  $h_P = 0.3 \text{ m}$  which has been measured in Altheim.

Figure 9a shows the load distribution under the track. The load is distributed on a wider area by the stiffness of the under-ballast plate. The thicker the plate is, the wider is the load distribution. The spatial distribution of the force density can be transformed into a time history by the train speed. Finally, the frequency content of this impact time history has been calculated and is presented in Figure 9b. The bandwidth of the spectrum is considerably reduced by the thicker plates. Figures 9c,d show the forces as one-third of octave band spectra for a single wheelset and for two wheelsets of a bogie with an axle distance of 2.5 m. It can be seen that in the most important frequency range up to 16 Hz, the effect of the plates is already present. At 12 Hz, the plate of  $h_P = 0.3 \text{ m}$  reduces the force

amplitude to one fourth compared to the standard ballast track. This agrees well with the observation of the measurement.

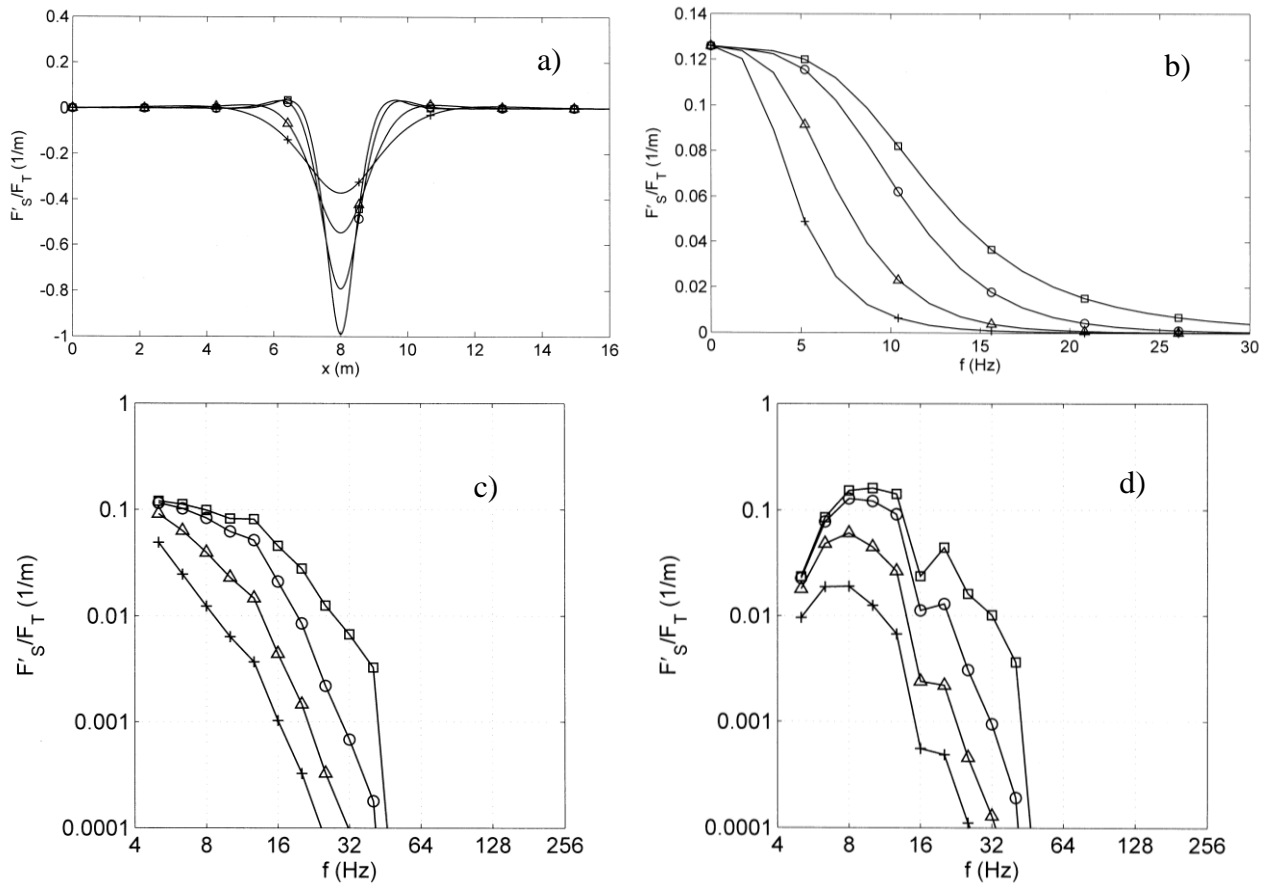


Figure 9: Calculated axle impulses for different under ballast plates,  $h_P = \square 0, \circ 0.15, \triangle 0.3, + 0.5$  m, a) load distribution along the track, b) impulse spectra on the ground, one-third octave band spectra of a single axle c), and of a bogie d).

## 6. Discussion of the reduction effect of the under-ballast plate

The impulses due to the passage of the static axle loads are superposed to a low-frequency quasi-static soil response [2, 8]. This quasi-static response attenuates strongly and is therefore restricted to the close near field of the track [2]. If the transmission of the axle impulses from different sleepers is irregular, for example due to a randomly varying ballast or soil stiffness, a scattered part of the impulses will be present in the far field [8, 9]. Both arguments together, the wider load distribution by the under-ballast plate and the scattering of the impulses by a randomly varying ballast or soil, explain well the observed reduction of the low-frequency ground vibration.

The dynamic reduction effect of an under-ballast plate is rather small and an amplification occurs at some resonance frequencies because of the reduced radiation damping [7, 10]. Other reasons for the low-frequency reduction could be a constrained settlement of the ballast, or the filtering of the sub-soil irregularities by the bending stiffness of the plate [11, 12].

## 7. Conclusion

For the Altheim site, different experimental methods have been presented which are useful for the prediction of train induced ground vibrations. The soil has been characterised by wave velocities or by transfer functions (mobilities) to predict the transmission. The track is characterised by its transfer function and the quasi-static compliance under the train load which are necessary to predict the vehicle-track interaction and the emission of ground vibration. From the track measurements, a high

portion of voided sleepers are concluded at this site. The train passages show a low-frequency reduction effect of the under-ballast plate compared to the standard ballast track. Calculations show the same reduction of the under-ballast plate for the axle-impulse spectrum. For a regular soil, this could only be seen in the near field of the track, but in case of a scattering of the axle impulses by an irregular soil with a randomly varying stiffness, this reduction can also be seen in the far-field as it has been measured in Altheim.

## REFERENCES

- 1 Jones, C. Use of numerical models to determine the effectiveness of anti-vibration system for railways, *Proceeding of the Institution of Civil Engineers, Transport*, **105**, 43-51, (1994).
- 2 Auersch, L. The use and validation of measured, theoretical and approximated point-load solutions for the prediction of train induced vibration in homogeneous and inhomogeneous soils. *International Journal of Acoustics and Vibrations*, **19**(1), 52-64, (2014).
- 3 Auersch, L., Said, S. Comparison of different dispersion evaluation methods and a case history with the inversion to a soil model, related admittance functions, and the prediction of train induced ground vibration, *Journal of Near Surface Geophysics* **13** (2), 127-142, (2015).
- 4 Auersch, L. Dynamics of the railway track and the underlying soil: the boundary-element solution, theoretical results and their experimental verification. *Vehicle System Dynamics*, **43** (9), 671-695, (2005).
- 5 Auersch, L., Said, S. Vibration measurements for the control of damaged and repaired railway tracks, *Proc. of the 7<sup>th</sup> Symposium on Environmental Vibration and Transportation Geodynamics*, Zhejiang University, Hangzhou, 28–30 October, (2016).
- 6 Auersch, L. Emission of train-induced ground vibration — Prediction of axle-load spectra and its experimental verification. *International Journal of Acoustics and Vibrations*, **22** (1), 74-83, (2017).
- 7 Auersch, L. Static and dynamic behaviours of isolated and un-isolated ballast tracks using a fast wavenumber domain method, *Archive of Applied Mechanics*, **87** (3), 555–574, (2017).
- 8 Auersch, L. Ground vibration due to railway traffic – The calculation of the effects of moving static loads and their experimental verification, *Journal of Sound and Vibration*, **293** (3-5), 599-610, (2006).
- 9 Huber, G. *Erschütterungsausbreitung beim Rad/Schiene-System*. Doctoral Thesis, University Karlsruhe, (1988).
- 10 Auersch, L. 2- and 3-dimensional methods for the assessment of ballast mats, ballast plates and other isolators of railway vibration. *International Journal of Acoustic and Vibration*, **11** (4), 167-176, (2006).
- 11 Hunt, H. Types of rail roughness and the selection of vibration isolation measures, *Proceedings of 9th International Workshop on Railway Noise and Vibration*, Munich, Germany, 4-8 September, (2007).
- 12 Auersch, L. Excitation of ground vibration due to the passage of trains over a track with trackbed irregularities and a varying support stiffness, *Vehicle System Dynamics* **53** (1), 1-29, (2015).